Computational and Applied Mathematics (2021) 40:22
https://doi.org/10.1007/s40314-020-01410-5

Numerical treatment of the space fractional advection–dispersion model arising in groundwater hydrology

H. Mesgarani[1] · J. Rashidinia[2] · Y. Esmaeelzade Aghdam[1] · O. Nikan[2]

Received: 24 May 2020 / Revised: 21 November 2020 / Accepted: 31 December 2020 /
Published online: 18 January 2021

Abstract
This paper studies a new computational method for the approximate solution of the space fractional advection–dispersion equation in sense of Caputo derivatives. In the first method, a time discretization is accomplished via the compact finite difference, while the fourth kind shifted Chebyshev polynomials are used to discretize the spatial derivative. The unconditional stability and convergence order of the method are studied via the energy method. Three examples are given for illustrating the effectiveness and accuracy of the new scheme when compared with existing numerical methods reported in the literature.

Keywords Space fractional advection–dispersion equation · Compact finite difference · Chebyshev collocation method · Error analysis

Mathematics Subject Classification 34K37 · 91G80 · 97N50

1 Introduction

Fractional calculus (FC) can be viewed as the generalization of classical calculus to non-integer orders (Podlubny 1998; Oldham and Spanier 1974; Milici et al. 2018). In recent years, FC has gained considerable popularity and importance in various fields of science

Communicated by Vasily E. Tarasov.

✉ Y. Esmaeelzade Aghdam
yonesesmaeelzade@gmail.com

H. Mesgarani
hmesgarani@sru.ac.ir

J. Rashidinia
rashidinia@iust.ac.ir

O. Nikan
omid_nikan@mathdep.iust.ac.ir; omidnikan77@yahoo.com

1 Department of Mathematics, Shahid Rajaee Teacher Training University, Tehran, Iran

2 School of Mathematics, Iran University of Science and Technology, Narmak, Tehran, Iran

Table 1 The parameters for advection–dispersion equation

Parameter	Description
R	Retardation factor
D_L	Longitudinal dispersion coefficient
D_e	Effective diffusion coefficient
α_L	Dynamic dispersivity
ν	Average flow velocity
C	Concentration of the tracer
ξ	Space coordinate
τ	Time coordinate

and engineering including economics, optimal control, materials, chemistry, physics, and social science (Ortigueira and Machado 2020; Tenreiro Machado and Lopes 2019; Rigi and Tajadodi 2019; Mahmoudi et al. 2019). In fact, due to the adequacy of fractional derivatives for capturing memory effects, many physical systems can be well described by means of fractional differential equations (Toubaei et al. 2019; Golbabai et al. 2019b, a; Nikan et al. 2020).

We consider the general advection–dispersion equation that is naturally utilized to explain the transient transport of solutes as

$$R\frac{\partial C(\xi,\tau)}{\partial \tau}=\left[D_L\frac{\partial^2}{\partial \xi^2}-\nu\frac{\partial}{\partial \xi}\right]C(\xi,\tau), \tag{1}$$

where $D_L = D_e + \alpha_L\nu$, $D_L > 0$, and $\nu > 0$. Table 1 lists the required parameters and variables for the equation (1).

Fractional space derivatives are applied for modeling anomalous diffusion or dispersion, where a particle spreads at a rate inconsistent with the classical Brownian motion model. The model (1) is based on the Fick's law, which describes the transport of passive tracers carried through a fluid flow in a porous medium (Liu et al. 2004). The FADE is a fundamental equation of motion that is used for modeling water flow movement (Hu et al. 2016), material transport and diffusion (Hernandez et al. 1995). For convenience and without losing the generality, let us introduce dimensionless space, time, and concentration variables by

$$x=\frac{\xi}{L},\qquad t=\frac{\tau}{L/\nu},\qquad u=\frac{C}{C_0},$$

respectively. Then the dimensionless advection–dispersion equation (ADE) can be rewritten as

$$\frac{\partial u(x,t)}{\partial t}=\gamma\frac{\partial^2 u(x,t)}{\partial x^2}-\mu\frac{\partial u(x,t)}{\partial x}\cdot, \tag{2}$$

where the constants γ and μ are the dispersion coefficient and the average fluid velocity, respectively. In virtue of the non-local importance of fractional derivatives, we suggest fractional order in Eq. (2) is used in the groundwater hydrology for modeling transport phenomena. The space fractional advection–dispersion equation (SFADE) is obtained from the classical equation by replacing the first-order and the second-order spatial derivatives by fractional derivatives termed in Caputo sense of order $\alpha \in (1, 2]$ and $\beta \in (0, 1]$, respectively. The SFADE is presented as

$$\frac{\partial u(x,t)}{\partial t}=\gamma\mathcal{D}_x^{\alpha}u(x,t)-\mu\mathcal{D}_x^{\beta}u(x,t)+q(x,t). \tag{3}$$

In addition, the advection–dispersion equation (ADE) of integer or fractional orders is widely utilized in environmental engineering and aviation (Liu et al. 2016), as well as in the marine (Farahani et al. 2015), chemical (Colla et al. 2015) and metallurgy (Zaib and Shafie 2014) areas. Therefore, the development of efficient numerical schemes for solving ADE is important both from the theoretical and practical point of views.

Hereafter we outline some preliminary concepts of fractional derivatives that are useful in the subsequent discussion (Podlubny 1998; Oldham and Spanier 1974; Milici et al. 2018).

Definition 1 The fractional derivative of Caputo type can be defined as

$$\mathcal{D}_x^{\beta} u(x,t) = \begin{cases} \frac{1}{\Gamma(n-\beta)} \int_0^x (x-\tau)^{n-\beta-1} \frac{\partial^n u(\tau,t)}{\partial \tau^n} \mathrm{d}\tau, & n-1 < \beta \le n \in \mathbb{N}, \\ \frac{\partial^n u(x,t)}{\partial x^n}, & \beta = n. \end{cases}$$

Remark 1 Some important properties of the Caputo derivative $\mathcal{D}_x^{\beta}$ are as listed:

1. $\mathcal{D}_x^{\beta} x^{\alpha} = \frac{\Gamma(1+\alpha)}{\Gamma(1+\alpha-\beta)} x^{\alpha-\beta}, \quad 0 < \beta < \alpha+1, \beta > -1,$
2. $\mathcal{D}_x^{\beta} (\gamma f(x,t) + \eta u(x,t)) = \gamma \mathcal{D}_x^{\beta} f(x,t) + \eta \mathcal{D}_x^{\beta} u(x,t),$
3. $\mathcal{D}_x^{\beta} \mathcal{D}_x^{n} u(x,t) = \mathcal{D}_x^{\beta+n} u(x,t) \neq \mathcal{D}_x^{n} \mathcal{D}_x^{\beta} u(x,t).$

In this article, we propose an numerical approach for computing the approximate solution of the SFADE as follows:

$$\frac{\partial u(x,t)}{\partial t} = \gamma \mathcal{D}_x^{\alpha} u(x,t) - \mu \mathcal{D}_x^{\beta} u(x,t) + q(x,t), \tag{4}$$

with the initial condition

$$u(x,0) = f(x), \quad 0 < x < L \tag{5}$$

and boundary conditions

$$u(0,t) = \upsilon_0(t), \quad u(L,t) = \upsilon_1(t), \quad 0 < t \le T, \tag{6}$$

in which $0 < \beta \le 1, \quad 1 < \alpha \le 2$.

Several numerical algorithms have been proposed for solving the SFADE. Ervin and Roop (2007) investigated an approach for FADE using the variational iteration method on bounded domain. Su et al. (2010) used the weighted average finite difference method. Khader and Sweilam (2014) adopted the Legendre collocation method. Saw and Kumar (2018, 2019) applied the Chebyshev collocation methods to obtain the approximation solution of the SFADE. Safdari et al. (2020a, b) adopted the spectral collocation method for solving SFADE. Aghdam et al. (2020) formulated a spectral collocation method to approximate SFADE.

The rest of this paper has the following organization. Section 2 presents the operational matrices of the fourth kind Chebyshev polynomials (FKCP) for fractional derivative. Section 3 describes the approximation of the fractional operator $\mathcal{D}_x^{\alpha} u(x,t)$ and implements the Chebyshev collocation approach to solve (4). The fourth kind shifted Chebyshev polynomials (FKSCP) and the compact finite difference are implemented to discretize the SFADE in the spatial and temporal variable, respectively. Section 4 discusses error analysis and upper bounds of time-discrete approach. Section 5 presents two numerical examples illustrating effectiveness and accuracy of the new scheme. Finally, Sect. 6 includes the main conclusions.

2 Some properties of the FKSCP

The FKCP $\mathcal{W}_i(x)$ defined in the domain $[-1, 1]$ are orthogonal polynomials of degree i as follows:

$$\mathcal{W}_i(x) = \frac{2^{2i}}{\binom{2i}{i}} P_i^{\left(\frac{1}{2}, \frac{-1}{2}\right)}(x),$$

where $P_i^{(r,s)}(x)$ is a Jacobi polynomial orthogonal corresponding to the weight function $\omega^{(r,s)}(x) = (1-x)^r(1+x)^s$ over $[-1, 1]$, such that

$$P_i^{(r,s)} = \frac{\Gamma(r+i+1)}{i!\Gamma(r+s+i+1)} \sum_{m=0}^{i} \binom{i}{m} \frac{\Gamma(r+s+i+m+1)}{\Gamma(r+m+1)} \times \left(\frac{x-1}{2}\right)^m.$$

$\mathcal{W}_i(x)$ can be organized

$$\mathcal{W}_i(x) = \mathfrak{I}_i \sum_{k=0}^{i-1} \sum_{\xi=0}^{k} \mathfrak{K}_{i,k,\xi} \times x^{k-\xi}, \quad x \in [-1, 1], \quad i = 1, 2, \ldots,$$

where

$$\mathfrak{I}_i = \frac{(2^{2i-2})\Gamma(i+0.5)(i-1)!}{(2i-2)!}, \quad \mathfrak{K}_{i,k,\xi} = \frac{(-1)^{\xi}\Gamma(i+k)}{2^k k! \times (i-k-1)\Gamma(k+1.5)} \times \binom{k}{\xi}.$$

The polynomials $\mathcal{W}_i(x)$ on $[-1, 1]$ corresponding to the weight function are orthogonal with the inner product as

$$\langle \mathcal{W}_m(x), \mathcal{W}_n(x) \rangle = \int_{-1}^{1} \sqrt{\frac{1-x}{1+x}} \mathcal{W}_m(x)\mathcal{W}_n(x)dx = \begin{cases} 0, & m \neq n, \\ \pi, & m = n. \end{cases}$$

In the domain $[0, 1]$, the SPCFK $\mathcal{W}_i^*(x) = \mathcal{W}_i(2x-1)$ can be defined as follows:

$$\mathcal{W}_i^*(x) = \mathfrak{I}_i \sum_{k=0}^{i-1} \sum_{\xi=0}^{k} \mathfrak{K}_{i,k,\xi} \times 2^k \times x^{k-\xi}, \quad x \in [0, 1], \quad i = 1, 2, \ldots \cdot$$

These polynomials are orthogonal in the domain $[0, 1]$ with respect to $\sqrt{\frac{1-x}{x}}$:

$$\langle \mathcal{W}_m^*(x), \mathcal{W}_n^*(x) \rangle = \int_{0}^{1} \sqrt{\frac{1-x}{x}} \mathcal{W}_m^*(x)\mathcal{W}_n^*(x)dx = \begin{cases} 0, & m \neq n, \\ \frac{\pi}{2}, & m = n. \end{cases}$$

Let $g(x)$ be a square-integrable function in $[0, 1]$. Then $g(x)$ may be extended in terms of $\mathcal{W}_i^*(x)$ as

$$g(x) = \sum_{i=0}^{N} c_i \mathcal{W}_i^*(x), \quad x \in [0, 1], \tag{7}$$

where the coefficients c_i, $i = 0, 1, \ldots, N$ are defied by

$$c_i = \frac{2}{\pi} \int_0^1 \sqrt{\frac{1-x}{x}} g(x)\mathcal{W}_{\mathrm{i}}^*(x)\mathrm{d}x. \tag{8}$$

The fractional derivative of $\mathcal{W}_i^*(x)$ is formulated based on the linearity of the Caputo definition

$$\mathcal{D}^{\omega}(\mathcal{W}_i^*(x)) = 0, \quad i = 0, 1, \ldots, \lceil\omega\rceil - 1, \quad \omega > 0, \tag{9}$$

where $\lceil\omega\rceil$ denotes the ceiling part of ω. The closed formulation of $\mathcal{D}^{\omega}(\mathcal{W}_i^*(x))$ can be written as

$$\mathcal{D}^{\omega}(\mathcal{W}_i^*(x)) = \sum_{k=0}^{i-\lceil\omega\rceil} \sum_{\xi=0}^{k} N_{i,k,\xi}^{\omega,\lceil\omega\rceil} \times x^{k-\xi-\omega+\lceil\omega\rceil}, \quad x \in [0,1], \quad i = 0, 1, \ldots, \tag{10}$$

and $N_{i,k,\xi}^{\omega,\lceil\omega\rceil}$ is defined by

$$N_{i,k,\xi}^{\omega,\lceil\omega\rceil} = \frac{2^{2i} \times (i)! \times \Gamma(i+0.5)}{(2i)! \times (i-k-\lceil\omega\rceil)! \times (k+\lceil\omega\rceil)!} \times \frac{\Gamma(i+k+\lceil\omega\rceil+1)}{\Gamma(k+\lceil\omega\rceil+1.5)} \times (-1)^{\xi} \times \binom{k+\lceil\omega\rceil}{\xi} \times \frac{\Gamma(k-\xi+\lceil\omega\rceil+1)}{\Gamma(k-\xi-\omega+\lceil\omega\rceil+1)}.$$

Using the properties listed in Remark 1 and combining Eqs. (7), (9) and (10), we have

$$\mathcal{D}^{\omega}(g(x)) = \sum_{i=\lceil\omega\rceil}^{N} \sum_{k=0}^{i-\lceil\omega\rceil} \sum_{\xi=0}^{k} c_i \times N_{i,k,\xi}^{\omega,\lceil\omega\rceil} \times x^{k-\xi-\omega+\lceil\omega\rceil}, \quad x \in [0,1]. \tag{11}$$

3 Numerical scheme

For discretizing (4), we consider the nodes $t_j = j\delta t$ $(j = 0, 1, \ldots, M)$ in the time domain $[0, T]$, where t_n satisfies $0 = t_0 < t_1 < \cdots < t_M = T$ with mesh length $\delta t = T/M$ for some positive integer M and define the collocation points $\{x_{r-1}\}_{r=1}^{N+1-\lceil\upsilon\rceil}$ using the roots of the SCPSK $U_{N+1-\lceil\upsilon\rceil}^*(x)$. Based on the Taylor formula of $u(x,t) \in \mathbb{C}^3(0,1)$, we have

$$\frac{\partial u(x_r, t_j)}{\partial t} = P_{\delta\tau} u(x_r, t_j) + \frac{\delta\tau}{2} \frac{\partial^2 u(x_r, t_j)}{\partial t^2} + \mathcal{O}(\delta\tau^2), \tag{12}$$

where $P_{\delta\tau} u(x_r, t_j) = \frac{u_r^j - u_r^{j-1}}{\delta\tau}$. Now, discretizing (4) in the grid points (x_r, t_j) and by substituting (12), it yields

$$P_{\delta\tau} u(x_r, t_j) + T_j = \gamma \frac{\partial^{\alpha} u(x_r, t_j)}{\partial x^{\alpha}} - \mu \frac{\partial^{\beta} u(x_r, t_j)}{\partial x^{\beta}} + q(x_r, t_j), \tag{13}$$

with

$$T_j = \frac{\delta\tau}{2} \frac{\partial^2 u(x_r, t_j)}{\partial t^2} + \mathcal{O}(\delta\tau^2)$$

and notice that

$$\frac{\partial^2 u(x_r, t_j)}{\partial t^2} = \gamma P_{\delta\tau} \frac{\partial^{\alpha} u(x_r, t_j)}{\partial x^{\alpha}} - \mu P_{\delta\tau} \frac{\partial^{\beta} u(x_r, t_j)}{\partial x^{\beta}} + P_{\delta\tau} q(x_r, t_j). \tag{14}$$

Substituting Eq. (14) in T_j and as well as in Eq. (13), one obtains

$$\begin{aligned} P_{\delta\tau} u(x_r, t_j) &= \gamma \frac{\partial^{\alpha} u(x_r, t_j)}{\partial x^{\alpha}} - \mu \frac{\partial^{\beta} u(x_r, t_j)}{\partial x^{\beta}} + q(x_r, t_j) \\ &\quad - \frac{\delta\tau}{2} \Big(\gamma P_{\delta\tau} \frac{\partial^{\alpha} u(x_r, t_j)}{\partial x^{\alpha}} - \mu P_{\delta\tau} \frac{\partial^{\beta} u(x_r, t_j)}{\partial x^{\beta}} + P_{\delta\tau} q(x_r, t_j) \Big) + \cdots . \end{aligned} \tag{15}$$

Let us define $u(x_r, t_j) = U_r^j$, $q(x_r, t_j) = q_r^j$. Then we get the semi-discrete scheme as

$$U_r^j - \frac{\delta\tau}{2}\gamma\frac{\partial^\alpha U_r^j}{\partial x^\alpha} + \frac{\delta\tau}{2}\mu\frac{\partial^\beta U_r^j}{\partial x^\beta} = U_r^{j-1} - \frac{\delta\tau}{2}\gamma\frac{\partial^\alpha U_r^{j-1}}{\partial x^\alpha} + \frac{\delta\tau}{2}\mu\frac{\partial^\beta U_r^{j-1}}{\partial x^\beta} + \frac{\delta\tau}{2}(q_r^j + q_r^{j-1}) + \mathcal{R}^j(x)\delta\tau^3, \tag{16}$$

where $\mathcal{R}^j(x)$ stands for a truncation term. It follows that, for fully discretizing (4), we need to approximate the Caputo derivative in $\frac{\partial^\alpha U_r^j}{\partial x^\alpha}$ and $\frac{\partial^\beta U_r^j}{\partial x^\beta}$ using the result of Eq. (11). In the Chebyshev collocation scheme, the approximate solution $u(x, t)$ can be represented as

$$u_N(x, t_j) = \sum_{i=0}^{N} \mathfrak{u}_i(t_j)\mathcal{W}_i^*(x). \tag{17}$$

In view of relations (11), (16) and (17), we have

$$\begin{aligned}
&\sum_{i=0}^{N} \mathfrak{u}_i^j\mathcal{W}_i^*(x) - \frac{\delta\tau}{2}\sum_{i=\lceil\alpha\rceil}^{N}\mathfrak{u}_i^j \times \left(\gamma\sum_{k=0}^{i-\lceil\alpha\rceil}\sum_{\xi=0}^{k} N_{i,k,\xi}^{\alpha,\lceil\alpha\rceil} \times x^{k-\xi-\alpha+\lceil\alpha\rceil}\right.\\
&\quad\left. + \mu\sum_{k=0}^{i-\lceil\beta\rceil}\sum_{\xi=0}^{k} N_{i,k,\xi}^{\beta,\lceil\beta\rceil} \times x^{k-\xi-\beta+\lceil\beta\rceil}\right)\\
&= \sum_{i=0}^{N} \mathfrak{u}_i^{j-1}\mathcal{W}_i^*(x) - \frac{\delta\tau}{2}\sum_{i=\lceil\alpha\rceil}^{N}\mathfrak{u}_i^{j-1} \times \left(\gamma\sum_{k=0}^{i-\lceil\alpha\rceil}\sum_{\xi=0}^{k} N_{i,k,\xi}^{\alpha,\lceil\alpha\rceil} \times x^{k-\xi-\alpha+\lceil\alpha\rceil}\right.\\
&\quad\left. + \mu\sum_{k=0}^{i-\lceil\beta\rceil}\sum_{\xi=0}^{k} N_{i,k,\xi}^{\beta,\lceil\beta\rceil} \times x^{k-\xi-\beta+\lceil\beta\rceil}\right)\\
&\quad + \frac{\delta\tau}{2}(q(x, t_j) + q(x, t_{j-1})),
\end{aligned} \tag{18}$$

where $\mathfrak{u}_i^j$ represents the coefficients at the point t_j. With the roots of the FKSCP, $\{x_r\}_{r=1}^{N+1-\lceil\upsilon\rceil}$, we collocate Eq. (18) as follows:

$$\begin{aligned}
&\sum_{i=0}^{N} \mathfrak{u}_i^j\mathcal{W}_i^*(x_r) - \frac{\delta\tau}{2}\sum_{i=\lceil\alpha\rceil}^{N}\mathfrak{u}_i^j \times \left(\gamma\sum_{k=0}^{i-\lceil\alpha\rceil}\sum_{\xi=0}^{k} N_{i,k,\xi}^{\alpha,\lceil\alpha\rceil} \times x_r^{k-\xi-\alpha+\lceil\alpha\rceil}\right.\\
&\quad\left. + \mu\sum_{k=0}^{i-\lceil\beta\rceil}\sum_{\xi=0}^{k} N_{i,k,\xi}^{\beta,\lceil\beta\rceil} \times x_r^{k-\xi-\beta+\lceil\beta\rceil}\right)\\
&= \sum_{i=0}^{N} \mathfrak{u}_i^{j-1}\mathcal{W}_i^*(x_r) - \frac{\delta\tau}{2}\sum_{i=\lceil\alpha\rceil}^{N}\mathfrak{u}_i^{j-1} \times \left(\gamma\sum_{k=0}^{i-\lceil\alpha\rceil}\sum_{\xi=0}^{k} N_{i,k,\xi}^{\alpha,\lceil\alpha\rceil} \times x_r^{k-\xi-\alpha+\lceil\alpha\rceil}\right.\\
&\quad\left. + \mu\sum_{k=0}^{i-\lceil\beta\rceil}\sum_{\xi=0}^{k} N_{i,k,\xi}^{\beta,\lceil\beta\rceil} \times x_r^{k-\xi-\beta+\lceil\beta\rceil}\right)\\
&\quad + \frac{\delta\tau}{2}(q(x_r, t_j) + q(x_r, t_{j-1})).
\end{aligned} \tag{19}$$

Substituting the boundary conditions given in Eq. (6) into (17), we obtain the $\lceil\upsilon\rceil$ equations

$$\sum_{i=0}^{N}(-1)^i\mathfrak{u}_i(t) = \upsilon_0(t), \qquad \sum_{i=0}^{N}(2i+1)\mathfrak{u}_i(t) = \upsilon_1(t). \tag{20}$$

Equation (19), together with $\lceil \nu \rceil$ equations of the boundary conditions (20) lead $N+1$ of algebraic equations that can be obtained the unknowns u_i, $i = 0, 1, \ldots, N$.

4 Error analysis

This section examines the time-discrete scheme in terms of unconditional stability and convergence issues. Assume that Ω represents an a bounded and open domain in $\mathbb{R}^2$. First, let us introduce the functional spaces endowed with standard norms and inner product

$$\langle u(x), v(x)\rangle = \int_{\Omega} u(x)v(x)\mathrm{d}x, \qquad u, v \in L_2(\Omega),$$

which induces the norm $\|u(x)\|_2 = \big\langle u(x), u(x)\big\rangle^{\frac{1}{2}}$ and let us define

$$H^s(\Omega) = \{u \in L_2(\Omega), \frac{\mathrm{d}^s u}{\mathrm{d}x^s} \in L_2(\Omega)\}.$$

Now, relation (16) can be rearranged according to the expression

$$\begin{aligned} &U^k - \frac{\delta\tau}{2}\Big(\gamma\, {}_a\mathcal{D}_x^{\alpha} U^k - \mu\, {}_a\mathcal{D}_x^{\beta} U^k\Big) \\ &\quad = U^{k-1} + \frac{\delta\tau}{2}\Big(\gamma\, {}_a\mathcal{D}_x^{\alpha} U^{k-1} - \mu\, {}_a\mathcal{D}_x^{\beta} U^{k-1}\Big) + \frac{\delta\tau}{2}(q^k + q^{k-1}), \qquad k = 1, 2, \ldots, M. \end{aligned} \tag{21}$$

We some lemmas that are introduced in the following (Ervin et al. 2007).

Lemma 1 *Assume that* $1 < \alpha < 2$. *Then for any* $u, v \in H^{\frac{\alpha}{2}}(\Omega)$ *it holds that*

$$\langle {}_a\mathcal{D}_x^{\alpha} u, v\rangle = \langle {}_a\mathcal{D}_x^{\frac{\alpha}{2}} u, {}_x\mathcal{D}_b^{\frac{\alpha}{2}} v\rangle, \quad \langle {}_x\mathcal{D}_b^{\alpha} u, v\rangle = \langle {}_x\mathcal{D}_b^{\frac{\alpha}{2}} u, {}_a\mathcal{D}_x^{\frac{\alpha}{2}} v\rangle.$$

Lemma 2 *Let* $\alpha > 0$ *be given. Then it follows that*

$$\langle {}_a\mathcal{D}_x^{\alpha} u, {}_x\mathcal{D}_b^{\alpha} u\rangle = \cos(\alpha\pi)\|{}_a\mathcal{D}_x^{\alpha} u\|^2_{L_2(\Omega)} = \cos(\alpha\pi)\|{}_x\mathcal{D}_b^{\alpha} u\|^2_{L_2(\Omega)}.$$

Now, we need to prove the following lemma:

Lemma 3 *For* $1 < \alpha \le 2$ *and the functions* $g(x), {}_a\mathcal{D}_x^{\alpha} g(x) \in H^{\alpha}(\Omega)$, *there exists a sufficiently small* $\delta\tau$ *such that*

$$\|g(x) + \frac{\delta\tau}{2}\, {}_a\mathcal{D}_x^{\alpha} g(x)\| \le \|g(x)\|.$$

Proof By virtue of the nature of the inner product, one can arrive at

$$\begin{aligned} \|g(x) + \frac{\delta\tau}{2}\, {}_a\mathcal{D}_x^{\alpha} g(x)\|^2 &\le \Big\langle g(x) + \frac{\delta\tau}{2}\, {}_a\mathcal{D}_x^{\alpha} g(x), g(x) + \frac{\delta\tau}{2}\, {}_a\mathcal{D}_x^{\alpha} g(x)\Big\rangle \\ &= \|g(x)\|^2 + \delta\tau\langle {}_a\mathcal{D}_x^{\frac{\alpha}{2}} g(x), {}_x\mathcal{D}_b^{\frac{\alpha}{2}} g(x)\rangle + \frac{\delta\tau^2}{4}\|{}_a\mathcal{D}_x^{\alpha} g(x)\|^2. \end{aligned}$$

From Lemma 2 and knowing that $1 < \alpha \le 2$, we obtain

$$\langle {}_a\mathcal{D}_x^{\frac{\alpha}{2}} g(x), {}_x\mathcal{D}_b^{\frac{\alpha}{2}} g(x)\rangle = \cos\Big(\frac{\alpha}{2}\pi\Big)\, \|{}_a\mathcal{D}_x^{\frac{\alpha}{2}} g(x)\|^2 < 0,$$

thus, by choosing a small enough $\delta\tau$ that guarantees

$$\langle {}_a\mathcal{D}_x^{\frac{\alpha}{2}} g(x), {}_x\mathcal{D}_a^{\frac{\alpha}{2}} g(x)\rangle + \frac{\delta\tau}{4}\|{}_a\mathcal{D}_x^{\alpha} g(x)\|^2 < 0.$$

Finally, we obtain

$$\|g(x) + \frac{\delta\tau}{2}{}_a\mathcal{D}_x^{\alpha} g(x)\|^2 \leq \|g(x)\|^2,$$

which proves the theorem. □

Lemma 4 *If $U^k \in H^1(\Omega)$, $k = 1, 2, \ldots, M$, and U^0 be the solution of the time-discretized scheme (21) and the initial condition, respectively, then*

$$\|U^k\| \leq \|U^0\| + \max_{0\leq r\leq N} \frac{\delta\tau}{2}(\|q_r^k\| + \|q_r^{k-1}\|). \tag{22}$$

Proof We will prove above result by principle of mathematical induction. First, when $k = 1$, we have

$$U^1 - \frac{\delta\tau}{2}\Big(\gamma\, {}_a\mathcal{D}_x^{\alpha} U^1 - \mu\, {}_a\mathcal{D}_x^{\beta} U^1\Big) = U^0 + \frac{\delta\tau}{2}\Big(\gamma\, {}_a\mathcal{D}_x^{\alpha} U^0 - \mu\, {}_a\mathcal{D}_x^{\beta} U^0\Big) + \frac{\delta\tau}{2}(q^1 + q^0). \tag{23}$$

Taking the inner product of Eq. (23) by U^1, one can obtain

$$\begin{aligned} &\|U^1\|^2 - \frac{\delta\tau}{2}\Big(\gamma\langle {}_a\mathcal{D}_x^{\alpha} U^1, U^1\rangle - \mu\langle {}_a\mathcal{D}_x^{\beta} U^1, U^1\rangle\Big)\\ &\quad = \langle U^0, U^1\rangle + \frac{\delta\tau}{2}\Big(\gamma\langle {}_a\mathcal{D}_x^{\alpha} U^0, U^1\rangle - \mu\langle {}_a\mathcal{D}_x^{\beta} U^0, U^1\rangle\Big)\\ &\quad\quad + \frac{\delta\tau}{2}(\langle q^1, U^1\rangle + \langle q^0, U^1\rangle). \end{aligned} \tag{24}$$

From Lemmas 1 and 2, it is clear that

$$\langle {}_a\mathcal{D}_x^{\alpha} U^1, U^1\rangle = \langle {}_a\mathcal{D}_x^{\frac{\alpha}{2}} U^1, {}_x\mathcal{D}_b^{\frac{\alpha}{2}} U^1\rangle = \cos\left(\frac{\alpha}{2}\pi\right)\|{}_a\mathcal{D}_x^{\frac{\alpha}{2}} U^1\|^2 \leq 0, \quad \forall\, 1 < \alpha \leq 2,$$

$$\langle {}_a\mathcal{D}_x^{\beta} U^1, U^1\rangle = \langle {}_a\mathcal{D}_x^{\frac{\beta}{2}} U^1, {}_x\mathcal{D}_b^{\frac{\beta}{2}} U^1\rangle = \cos\left(\frac{\beta}{2}\pi\right)\|{}_a\mathcal{D}_x^{\frac{\beta}{2}} U^1\|^2 \geq 0, \quad \forall\, 0 < \beta \leq 1.$$

Regarding Lemma 3 and the Schwarz inequality, we have

$$\langle U^0, U^1\rangle + \frac{\delta\tau}{2}\langle {}_a\mathcal{D}_x^{\alpha} U^0, U^1\rangle = \langle U^0 + \frac{\delta\tau}{2}{}_a\mathcal{D}_x^{\alpha} U^0, U^1\rangle \leq \|U^0 + \frac{\delta\tau}{2}{}_a\mathcal{D}_x^{\alpha} U^0\|\|U^1\| \leq \|U^0\|\|U^1\|.$$

The aforesaid relation can be rewritten as

$$\|U^1\| \leq \|U^0\| + \max_{0\leq r\leq N}\frac{\delta\tau}{2}(\|q_r^1\| + \|q_r^0\|).$$

Suppose that the theorem is true for all j

$$\|U^j\| \leq \|U^0\| + \max_{0\leq r\leq N}\frac{\delta\tau}{2}(\|q_r^j\| + \|q_r^{j-1}\|), \quad j = 1, 2, \ldots, k-1.$$

Taking the inner product of Eq. (23) by U^k, we have

$$\begin{aligned} &\|U^k\|^2 - \frac{\delta\tau}{2}\Big(\gamma\langle {}_a\mathcal{D}_x^{\alpha} U^k, U^k\rangle - \mu\langle {}_a\mathcal{D}_x^{\beta} U^k, U^k\rangle\Big)\\ &\quad = \langle U^{k-1}, U^k\rangle + \frac{\delta\tau}{2}\Big(\gamma\langle {}_a\mathcal{D}_x^{\alpha} U^{k-1}, U^k\rangle - \mu\langle {}_a\mathcal{D}_x^{\beta} U^{k-1}, U^k\rangle\Big)\\ &\quad\quad + \frac{\delta\tau}{2}(\langle q^k, U^k\rangle + \langle q^{k-1}, U^k\rangle). \end{aligned}$$

From the Schwarz inequality and $U^k \in H^1(\Omega)$, we have the following inequality:

$$\|U^k\| \leq \|U^{k-1}\| + \max_{0\leq r\leq N} \frac{\delta\tau}{2}(\|q_r^k\| + \|q_r^{k-1}\|).$$

Therefore, Lemma 4 is proven by induction on k. □

Next theorem proves the stability of relation (16).

Theorem 1 *The time semi-discretization* (16) *is unconditionally stable.*

Proof Let us consider that $\widehat{U}_r^j$, $j = 1, 2, \ldots, M$, is an approximate solution of (16), with the initial condition $\widehat{U}_r^0 = u(x, 0)$. Then the error $\varepsilon^j = U_r^j - \widehat{U}_r^j$ satisfies

$$\varepsilon^j - \frac{\delta\tau}{2}\big(\gamma_a \mathcal{D}_x^\alpha \varepsilon^j - \mu_a \mathcal{D}_x^\beta \varepsilon^j\big) = \varepsilon^{j-1} + \frac{\delta\tau}{2}\big(\gamma_a \mathcal{D}_x^\alpha \varepsilon^{j-1} - \mu_a \mathcal{D}_x^\beta \varepsilon^{j-1}\big).$$

Using the aforesaid equation and Lemma 4, it follows that

$$\|\varepsilon^j\| \leq \|\varepsilon^0\|, \quad j = 1, 2, \ldots, M.$$

This shows that the scheme (16) is unconditionally stable. □

Theorem 2 *Let* $\varepsilon^j = u(x, t_j) - U^j$, $j = 1, 2, \ldots, M$, *be the errors associated with Eq.* (16). *Then we obtain that*

$$\|\varepsilon^j\| \leq C_x \delta\tau^2,$$

where $C_x > 0$ *is depends on* x.

Proof First, we obtain the following weak form using Eq. (16) as

$$\begin{aligned}\|\varepsilon^j\|^2 - \frac{\delta\tau}{2}\big(\gamma\langle {}_a\mathcal{D}_x^\alpha \varepsilon^j, \varepsilon^j\rangle - \mu\langle {}_a\mathcal{D}_x^\beta \varepsilon^j, \varepsilon^j\rangle\big) &= \langle \varepsilon^{j-1}, \varepsilon^j\rangle + \frac{\delta\tau}{2}\big(\gamma\langle {}_a\mathcal{D}_x^\alpha \varepsilon^{j-1}, \varepsilon^j\rangle \\ &\quad - \mu\langle {}_a\mathcal{D}_x^\beta \varepsilon^{j-1}, \varepsilon^j\rangle\big) + \delta\tau^3\langle \mathcal{R}^j(x), \varepsilon^j\rangle.\end{aligned}$$

for $j = 1, 2, \ldots, M$.
Based on the Lemmas 1, 2 ,3 and Cauchy–Schwarz inequality, we conclude that

$$\|\varepsilon^j\|^2 \leq \|\varepsilon^{j-1}\|\|\varepsilon^j\| + (\delta\tau)^3\|\mathcal{R}^j(x)\|\|\varepsilon^j\|.$$

So, one can get

$$\|\varepsilon^j\| - \|\varepsilon^{j-1}\| \leq (\delta\tau)^3\|\mathcal{R}^j(x)\|, \quad \Longrightarrow \|\varepsilon^j\| - \|\varepsilon^{j-1}\| \leq C(\delta\tau)^3. \tag{25}$$

Summing for j from 1 to M, we obtain

$$\sum_{j=1}^{M}\Big(\|\varepsilon^j\| - \|\varepsilon^{j-1}\|\Big) \leq \sum_{j=1}^{M} C(\delta\tau)^3.$$

From the above relation, we can conclude

$$\|\varepsilon^M\| - \|\varepsilon^0\| \leq CM(\delta\tau)^3,$$

since $\|\varepsilon^0\| = 0$ and $\delta\tau = \frac{T}{M}$, we have

$$\|\varepsilon^M\| \leq C_x \delta\tau^2,$$

where $C_x = CT$. The proof of Theorem 2 is completed. □

Table 2 The maximum norm error L_∞ obtained with the proposed method and those in Khader and Sweilam (2014); Saw and Kumar (2018, 2019) with $\alpha = 2$, $\beta = 1$, $N = 3$ and $M = 400$ at $T = 1$ for Example 1

x	Khader and Sweilam (2014)	Saw and Kumar (2018)	Saw and Kumar (2019)	Proposed method
0	4.48378×10^{-3}	2.19788×10^{-5}	2.19788×10^{-5}	1.30104×10^{-18}
0.1	4.47966×10^{-3}	2.41687×10^{-5}	2.41687×10^{-5}	2.22286×10^{-9}
0.2	4.20132×10^{-3}	2.60334×10^{-5}	2.60333×10^{-5}	4.35339×10^{-9}
0.3	3.69517×10^{-3}	2.75122×10^{-5}	2.75122×10^{-5}	6.24096×10^{-9}
0.4	3.00756×10^{-3}	2.85448×10^{-5}	2.85448×10^{-5}	7.73497×10^{-9}
0.5	2.18488×10^{-3}	2.90705×10^{-5}	2.90705×10^{-5}	8.68481×10^{-9}
0.6	1.27351×10^{-3}	2.90289×10^{-5}	2.90289×10^{-5}	8.93986×10^{-9}
0.7	0.31983×10^{-3}	2.83595×10^{-5}	2.83594×10^{-5}	8.34952×10^{-9}
0.8	0.62979×10^{-3}	2.70016×10^{-5}	2.70016×10^{-5}	6.76317×10^{-9}
0.9	1.52897×10^{-3}	2.48949×10^{-5}	2.48949×10^{-5}	4.03020×10^{-9}
1.0	2.33134×10^{-3}	2.19787×10^{-5}	2.19788×10^{-5}	0

5 Numerical examples

In this section, we present the numerical results of the proposed method on three test problems. Moreover, we will test the accuracy of proposed method for different values of N, M at final times T. In addition, the computational order (denoted by $C_{\delta\tau}$) is computed by the formula

$$C_{\delta\tau} = \frac{\log\left(\frac{E_1}{E_2}\right)}{\log\left(\frac{\delta\tau_1}{\delta\tau_2}\right)},$$

where E_1 and E_2 are the errors corresponding to grids with time steps $\delta\tau_1$ and $\delta\tau_2$, respectively.

Example 1 Consider the following SFADE

$$\frac{\partial u(x,t)}{\partial t} = \frac{\partial^\alpha u(x,t)}{\partial x^\alpha} - \frac{\partial^\beta u(x,t)}{\partial x^\beta} + e^{-2t}\left(2(x^\beta - x^\alpha) - \alpha! + \frac{\Gamma(\alpha+1)}{\Gamma(\alpha-\beta+1)}x^{\alpha-\beta} - \beta!\right)$$

with boundary and initial conditions

$$u(x,0) = x^\alpha - x^\beta,$$
$$u(0,t) = u(1,t) = 0.$$

The analytical solution of this problem is $u(x,t) = e^{-2t}(x^\alpha - x^\beta)$.

Tables 2–6 list the results for Example 1, with various values of M and N at different values of T. Tables 2 and 3 make a comparison between the obtained results with the techniques described in (Khader and Sweilam 2014; Saw and Kumar 2018, 2019) at $T = 1$ and $T = 2$. We verify that the proposed method achieves superior accuracy than the techniques described in (Khader and Sweilam 2014; Saw and Kumar 2019, 2018). Table 4 includes the maximum norm error L_∞ yielded by the proposed method for $N = 5$ and various values of M, at $T = 1$. Table 5 reports that the computational order of the method in the time variable is approximately $\mathcal{O}(\delta\tau^2)$ which is in accordance with the theoretical results. Table 6 demonstrates the

Table 3 The maximum norm error L_∞ with the proposed method and those in Khader and Sweilam (2014); Saw and Kumar (2018, 2019) with $\alpha = 2$, $\beta = 1$, $M = 400$ and $N = 5$ at $T = 2$ for Example 1

x	Khader and Sweilam (2014)	Saw and Kumar (2018)	Saw and Kumar (2019)	Proposed method
0	2.72649×10^{-5}	2.19788×10^{-5}	2.19788×10^{-5}	1.37146×10^{-18}
0.1	3.45589×10^{-5}	2.41644×10^{-5}	2.41644×10^{-5}	2.59266×10^{-9}
0.2	3.80967×10^{-5}	2.60588×10^{-5}	2.60588×10^{-5}	5.12222×10^{-9}
0.3	3.80910×10^{-5}	2.75808×10^{-5}	2.75808×10^{-5}	7.30415×10^{-9}
0.4	3.51428×10^{-5}	2.86516×10^{-5}	2.86516×10^{-5}	8.89583×10^{-9}
0.5	3.00926×10^{-5}	2.91965×10^{-5}	2.91965×10^{-5}	9.70550×10^{-9}
0.6	2.38712×10^{-5}	2.91470×10^{-5}	2.91470×10^{-5}	9.60120×10^{-9}
0.7	1.73512×10^{-5}	2.84434×10^{-5}	2.84434×10^{-5}	8.51976×10^{-9}
0.8	1.11982×10^{-5}	2.70362×10^{-5}	2.70362×10^{-5}	6.47569×10^{-9}
0.9	0.57215×10^{-5}	2.48887×10^{-5}	2.48887×10^{-5}	3.57017×10^{-9}
1.0	0.07256×10^{-5}	2.19788×10^{-5}	2.19788×10^{-5}	1.11172×10^{-18}

Table 4 The maximum norm error L_∞ obtained with the proposed method with $N = 5$ at $T = 1$ of Example 1

x	$M = 100$	$M = 200$	$M = 400$	$M = 800$	$M = 1600$
0	9.92807×10^{-18}	1.24162×10^{-17}	9.52764×10^{-18}	1.12178×10^{-17}	8.27644×10^{-18}
0.1	7.66048×10^{-8}	1.91519×10^{-8}	4.78800×10^{-9}	1.19700×10^{-9}	2.99251×10^{-10}
0.2	1.51345×10^{-7}	3.78375×10^{-8}	9.45946×10^{-9}	2.36487×10^{-9}	5.91218×10^{-10}
0.3	2.15813×10^{-7}	5.39551×10^{-8}	1.34889×10^{-8}	3.37223×10^{-9}	8.43058×10^{-10}
0.4	2.62841×10^{-7}	6.57124×10^{-8}	1.64282×10^{-8}	4.10707×10^{-9}	1.02677×10^{-9}
0.5	2.86762×10^{-7}	7.16930×10^{-8}	1.79234×10^{-8}	4.48056×10^{-9}	1.12022×10^{-9}
0.6	2.83680×10^{-7}	7.09224×10^{-8}	1.77307×10^{-8}	4.43270×10^{-9}	1.10817×10^{-9}
0.7	2.51726×10^{-7}	6.29338×10^{-8}	1.57336×10^{-8}	3.93340×10^{-9}	9.83351×10^{-10}
0.8	1.91332×10^{-7}	4.78345×10^{-8}	1.19587×10^{-8}	2.98969×10^{-9}	7.47423×10^{-10}
0.9	1.05485×10^{-7}	2.63721×10^{-8}	6.59308×10^{-9}	1.64827×10^{-9}	4.12069×10^{-10}
1.0	1.29780×10^{-17}	4.51945×10^{-19}	2.70462×10^{-17}	1.12495×10^{-18}	4.24973×10^{-17}

computational order at the final times $T \in \{2, 10\}$. Figure 1 illustrates the numerical solution and the maximum norm error L_∞ with $N = 7$ and $M = 400$ at $T = 1$. Figure 2 draws the behaviour of the maximum norm errors L_∞ when adopting $N = 3$ and $N = 7$ for various values of M at $T = 2$. Figure 3a includes the behaviour of the maximum norm error L_∞ and L_2-norm when choosing $M = 400$, and various values N at $T = 1$. Figure 3b plots the maximum norm error L_∞ for $N = 5$ and various values M at $T = 1$. Figure 4 represents the behaviour of the maximum norm errors L_∞ for different values of $\{\alpha, \beta\}$, at $T = 1$.

Example 2 Consider the following SFADE

$$\frac{\partial u(x,t)}{\partial t} = \frac{\partial^{1.5} u(x,t)}{\partial x^{1.5}} - 2\frac{\partial u(x,t)}{\partial x} + x(x-1)(2t-1) + 2t(t-1)(2x-1) - \frac{4\sqrt{x}t(t-1)}{\sqrt{\pi}}, \tag{26}$$

Table 5 The maximum norm error L_∞, computational orders and CPU time with $N = 7$ at $T = 1$ for Example 1

M	$N = 7$				
	L_∞	$C_{\delta\tau}$	L_2	$C_{\delta\tau}$	CPU time
100	2.86772×10^{-7}		6.46683×10^{-7}		7.34264
200	7.16954×10^{-8}	1.99995	1.61676×10^{-7}	1.99995	9.53502
400	1.79240×10^{-8}	1.99999	4.04194×10^{-8}	1.99999	11.05831
800	4.48101×10^{-9}	2.00000	1.01049×10^{-8}	2.00000	14.80701
1600	1.12025×10^{-9}	2.00000	2.52622×10^{-9}	2.00000	17.07253

Table 6 The maximum norm error L_∞ and computational orders with $N = 3$ at the final times $T \in \{2, 10\}$ for Example 1

	M	$N = 7$				CPU time
		L_∞	$C_{\delta\tau}$	L_2	$C_{\delta\tau}$	
$T = 2$	100	1.43012×10^{-7}		3.23805×10^{-7}		2.15304
	200	3.57582×10^{-8}	1.99979	8.09629×10^{-8}	1.99979	3.04520
	400	8.93986×10^{-9}	1.99995	2.02415×10^{-8}	1.99995	4.60738
	800	2.23499×10^{-9}	1.99870	5.06041×10^{-9}	1.99999	7.50869
	1600	5.58748×10^{-10}	1.99999	1.26511×10^{-9}	2.00000	10.8204
T=10	100	4.00498×10^{-13}		9.06805×10^{-13}		2.57012
	200	1.00485×10^{-13}	1.99481	2.27517×10^{-13}	1.99482	3.15760
	400	2.51440×10^{-14}	1.99870	5.69305×10^{-14}	1.99870	4.90863
	800	6.28741×10^{-15}	1.99967	1.42358×10^{-14}	1.99968	7.91053
	1600	1.57194×10^{-15}	1.99992	3.55916×10^{-15}	1.99992	11.3501

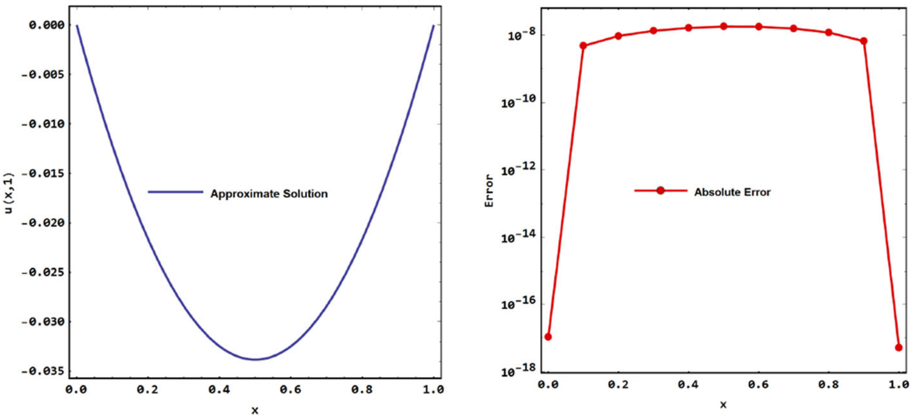

Fig. 1 The approximate solution (left panel) and the maximum norm error L_∞ (right panel) with $M = 400$ and $N = 7$ at $T = 1$ for Example 1

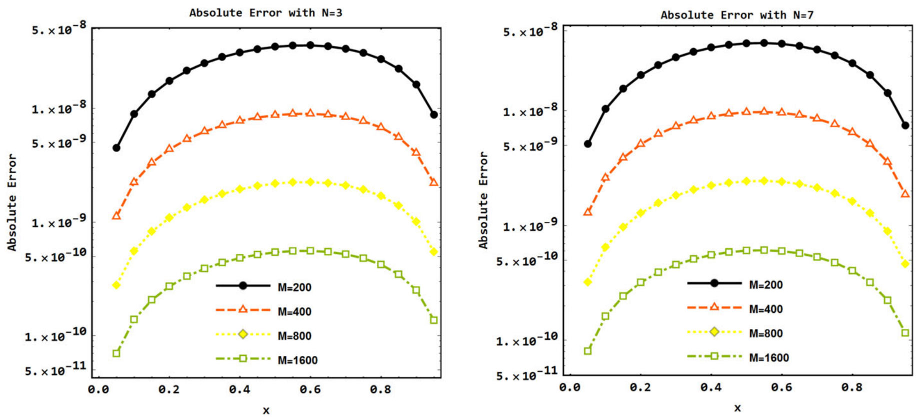

Fig. 2 The maximum error norms L_∞ with $\{\alpha = 1.9, \beta = 1\}$ and different values of N and M at $T = 2$ for Example 1

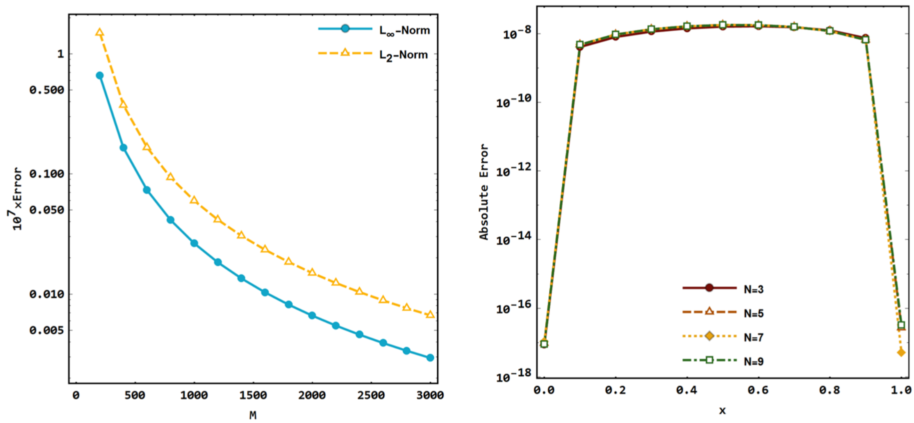

(a) The maximum norm errors L_∞ with $\{\alpha = 1.9, \beta = 0.9\}$ and $N = 3$ at $T = 1$ for Example 1.

(b) The maximum norm error L_∞ with $\{\alpha = 1.9, \beta = 0.9\}$, and $M = 400$ and $N \in \{3, 5, 7, 9\}$ at $T = 1$ for Example 1.

Fig. 3 **a** The maximum norm errors L_∞ with $\{\alpha = 1.9, \beta = 0.9\}$ and $N = 3$ at $T = 1$ for Example 1. **b** The maximum norm error L_∞ with $\{\alpha = 1.9, \beta = 0.9\}$, and $M = 400$ and $N \in \{3, 5, 7, 9\}$ at $T = 1$ for Example 1

with boundary and initial conditions

$$u(x, 0) = 0, \quad u(0, t) = u(1, t) = 0, \quad t > 0, \tag{27}$$

such that the analytical solution is $u(x, t) = xt(x - 1)(t - 1)$.

Table 7 makes the comparison between the numerical and the analytical solutions for various values of $T \in \{0.3, 06, 0.9\}$, showing that the method rapidly converges to the analytical solution. Figure 5 plots the behaviour of the maximum norm error for different values of $\{\alpha, \beta\}$ at $T = 10$.

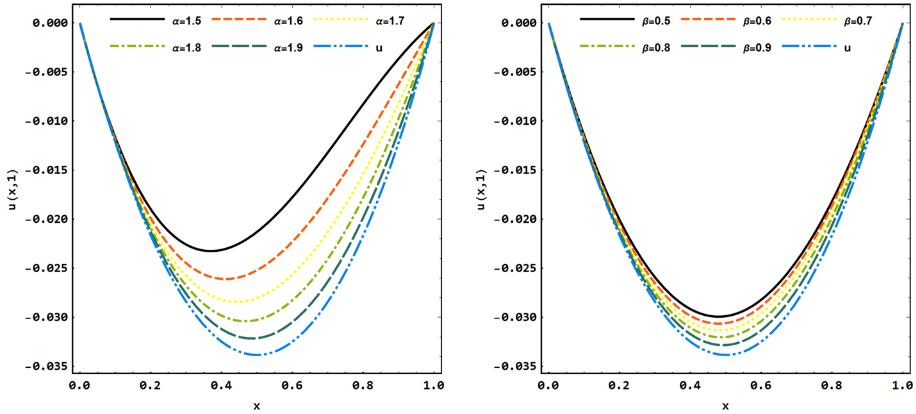

Fig. 4 The behavior of the approximate solutions for $\alpha \in \{1.5, 1.6, 1.7, 1.8, 1.9\}$, $\beta = 1$ (left panel) and $\beta \in \{0.5, 0.6, 0.7, 0.8, 0.9\}$, $\alpha = 1.5$ (right panel) for Example 1

Table 7 The analytical and approximate solutions with $\alpha = 1.5$ and $\beta = 1$ at various values of $T \in \{0.3, 0.6, 0.9\}$ of Example 2

x	$u_e(x, 0.3)$	$u_n(x, 0.3)$	$u_e(x, 0.6)$	$u_n(x, 0.6)$	$u_e(x, 0.9)$	$u_n(x, 0.9)$
0	0	0	0	0	0	0
0.1	0.0189	0.0189	0.0216	0.0216	0.0081	0.0081
0.2	0.0336	0.0336	0.0384	0.0384	0.0144	0.0144
0.3	0.0441	0.0441	0.0504	0.0504	0.0189	0.0189
0.4	0.0504	0.0504	0.0576	0.0576	0.0216	0.0216
0.5	0.0525	0.0525	0.0600	0.0600	0.0225	0.0225
0.6	0.0504	0.0504	0.0576	0.0576	0.0216	0.0216
0.7	0.0441	0.0441	0.0504	0.0504	0.0189	0.0189
0.8	0.0336	0.0336	0.0384	0.0384	0.0144	0.0144
0.9	0.0189	0.0189	0.0216	0.0216	0.0081	0.0081
1.0	0	0	0	0	0	0

Example 3 Consider the following SFADE

$$\frac{\partial u(x,t)}{\partial t} = \Gamma(1.8)x^{1.2} \times \frac{\partial^{1.2} u(x,t)}{\partial x^{1.2}} - \Gamma(2.8)x^{0.2} \times \frac{\partial^{0.2} u(x,t)}{\partial x^{0.2}} - (x^2 - x^3)\sin(t) - 6x^3\cos(t)\left(\frac{\Gamma(2.8)}{\Gamma(3.8)} - \frac{\Gamma(1.8)}{\Gamma(2.8)}\right), \tag{28}$$

with boundary and initial conditions

$$u(x, 0) = x^2 - x^3, \quad u(0, t) = u(1, t) = 0, \quad t > 0, \tag{29}$$

which the analytical solution is $u(x, t) = (x^2 - x^3)\cos(t)$.

Table 8 demonstrates the computational order at the final times $T \in \{1, 2\}$ which is in accordance with the theoretical results.

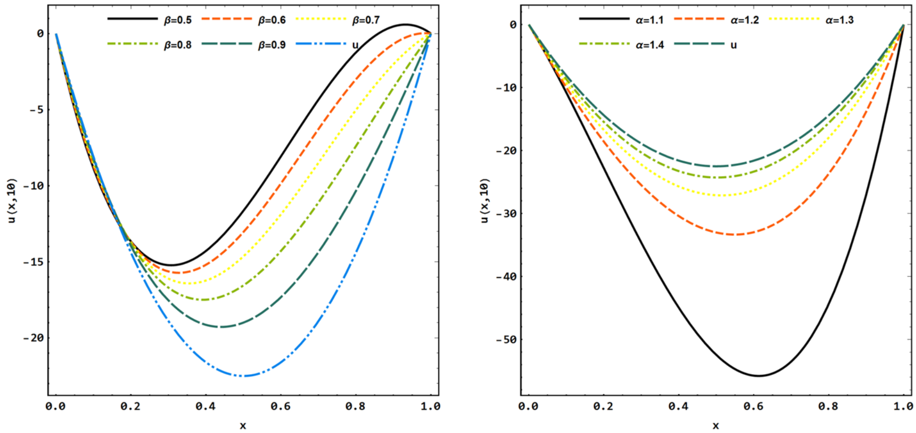

Fig. 5 The approximate solutions of Example 2 for $\beta \in \{0.5, 0.6, 0.7, .8, 0.9\}$, $\alpha = 1$ (left panel) and $\alpha \in \{1.1, 1.2, 1.3, 1.4\}$, $\beta = 1$ (right panel) at final time $T = 10$

Table 8 The maximum norm error L_∞ and computational orders with $N = 5$ the final times $T \in \{1, 2\}$ for Example 3

	M	$N = 5$				CPU time
		L_∞	$C_{\delta\tau}$	L_2	$C_{\delta\tau}$	
$T = 1$	10	2.59787×10^{-5}		5.30970×10^{-5}		1.57071
	20	6.49462×10^{-6}	2.00001	1.32746×10^{-5}	1.99996	2.02579
	40	1.62365×10^{-6}	2.00000	3.31866×10^{-6}	1.99999	3.01237
	80	4.05912×10^{-7}	2.00000	8.29667×10^{-7}	2.00000	4.50421
	160	1.01478×10^{-7}	2.00000	2.07417×10^{-7}	2.00000	6.96402
	320	2.53695×10^{-8}	2.00000	5.18542×10^{-8}	2.00000	8.02486
$T = 2$	10	1.63619×10^{-4}		3.39673×10^{-4}		1.62140
	20	4.08041×10^{-5}	2.00355	8.46956×10^{-5}	2.00379	2.29706
	40	1.01948×10^{-5}	2.00089	2.11600×10^{-5}	2.00095	3.40972
	80	2.54830×10^{-6}	2.00022	5.28913×10^{-6}	2.00024	4.80439
	160	6.37050×10^{-7}	2.00006	1.32223×10^{-6}	2.00006	6.20796
	320	1.59261×10^{-7}	2.00001	3.30554×10^{-7}	2.00001	8.59014

6 Conclusion

This paper proposed a new method for solving the SFADE. The numerical algorithm involves two steps. First, the compact finite difference is applied to discretize the time derivative. Second, the FKSCP is implemented to approximate the space fractional derivatives. The error analysis of the proposed method was investigated in L^2 space. To illustrate the applicability and validity of the new scheme, illustrative examples were provided. The numerical results verify well the theoretical analysis.

Acknowledgements The authors are thankful to the respected reviewers for their valuable comments and constructive suggestions towards the improvement of the original paper. The authors are also very grateful to the Associate Editor, Professor Vasily E. Tarasov for managing the review process.

References

Aghdam YE, Mesgrani H, Javidi M, Nikan O (2020) A computational approach for the space-time fractional advection-diffusion equation arising in contaminant transport through porous media. Eng Comput. https://doi.org/10.1007/s00366-020-01021-y

Colla L, Fedele L, Buschmann M (2015) Laminar mixed convection of TiO2-water nanofluid in horizontal uniformly heated pipe flow. Int J Therm Sci 97:26–40

Ervin VJ, Roop JP (2007) Variational solution of fractional advection dispersion equations on bounded domains in 1d. Numer Methods Partial Differ Equ Int J 23(2):256–281

Ervin VJ, Heuer N, Roop JP (2007) Numerical approximation of a time dependent, nonlinear, space-fractional diffusion equation. SIAM J Numer Anal 45(2):572–591

Farahani A, Taghaddos H, Shekarchi M (2015) Prediction of long-term chloride diffusion in silica fume concrete in a marine environment. Cement Con Compos 59:10–17

Golbabai A, Nikan O, Nikazad T (2019a) Numerical analysis of time fractional Black–Scholes European option pricing model arising in financial market. Comput Appl Math 38(4):173

Golbabai A, Nikan O, Nikazad T (2019b) Numerical investigation of the time fractional mobile-immobile advection-dispersion model arising from solute transport in porous media. Int J Appl Comput Math 5(3):50

Hernandez J, Crespo A, Duijm N (1995) Numerical modeling of turbulent jet diffusion flames in the atmospheric surface layer. Combust flame 101(1–2):113–131

Hu G, Zhao L, Wu X, Li R, Wu T, Xie C, Qiao Y, Shi J, Li W, Cheng G (2016) New Fourier-series-based analytical solution to the conduction–convection equation to calculate soil temperature, determine soil thermal properties, or estimate water flux. Int J Heat Mass Transfer 95:815–823

Khader M, Sweilam N (2014) Approximate solutions for the fractional advection-dispersion equation using legendre pseudo-spectral method. Comput Appl Math 33(3):739–750

Liu F, Anh V, Turner I (2004) Numerical solution of the space fractional Fokker–Planck equation. J Comput Appl Math 166(1):209–219

Liu L, Zheng L, Liu F, Zhang X (2016) Anomalous convection diffusion and wave coupling transport of cells on comb frame with fractional Cattaneo–Christov flux. Commun Nonlinear Sci Numer Simul 38:45–58

Mahmoudi M, Ghovatmand M, Jafari H (2019) An adaptive collocation method for solving delay fractional differential equations. Int J Appl Comput Math 5(6):157

Milici C, Drăgănescu G, Machado JT (2018) Introduction to fractional differential equations, vol 25. Springer, Berlin

Nikan O, Machado JT, Golbabai A (2020) Numerical solution of time-fractional fourth-order reaction-diffusion model arising in composite environments. Appl Math Model 89:819–836

Oldham KB, Spanier J (1974) The fractional calculus, vol. 111 of Mathematics in science and engineering

Ortigueira MD, Machado JT (2020) On the properties of some operators under the perspective of fractional system theory. Commun Nonlinear Sci Numer Simul 82:105022

Podlubny I (1998) Fractional differential equations: an introduction to fractional derivatives, fractional differential equations, to methods of their solution and some of their applications, vol 198. Elsevier, Amsterdam

Rigi F, Tajadodi H (2019) Numerical approach of fractional Abel differential equation by Genocchi polynomials. Int J Appl Comput Math 5(5):134

Safdari H, Mesgarani H, Javidi M, Aghdam YE (2020b) Convergence analysis of the space fractional-order diffusion equation based on the compact finite difference scheme. Comput Appl Math 39(2):1–15

Safdari H, Aghdam YE, Gómez-Aguilar J (2020a) Shifted Chebyshev collocation of the fourth kind with convergence analysis for the space-time fractional advection–diffusion equation. Eng Comput. https://doi.org/10.1007/s00366-020-01092-x

Saw V, Kumar S (2018) Fourth kind shifted Chebyshev polynomials for solving space fractional order advection-dispersion equation based on collocation method and finite difference approximation. Int J Appl Comput Math 4(3):82

Saw V, Kumar S (2019) Second kind Chebyshev polynomials for solving space fractional advection-dispersion equation using collocation method. Iran J Sci Technol Trans A Sci 43(3):1027–1037

Su L, Wang W, Xu Q (2010) Finite difference methods for fractional dispersion equations. Appl Math Comput 216(11):3329–3334

Tenreiro Machado JA, Lopes AM (2019) Fractional-order kinematic analysis of biomechanical inspired manipulators. J Vibrat Control: 102–111

Toubaei S, Garshasbi M, Reihani P (2019) Boundary functions determination in an inverse time fractional heat conduction problem. Comput Appl Math 38(4):190

Zaib A, Shafie S (2014) Thermal diffusion and diffusion thermo effects on unsteady mhd free convection flow over a stretching surface considering joule heating and viscous dissipation with thermal stratification, chemical reaction and hall current. J Franklin Inst 351(3):1268–1287